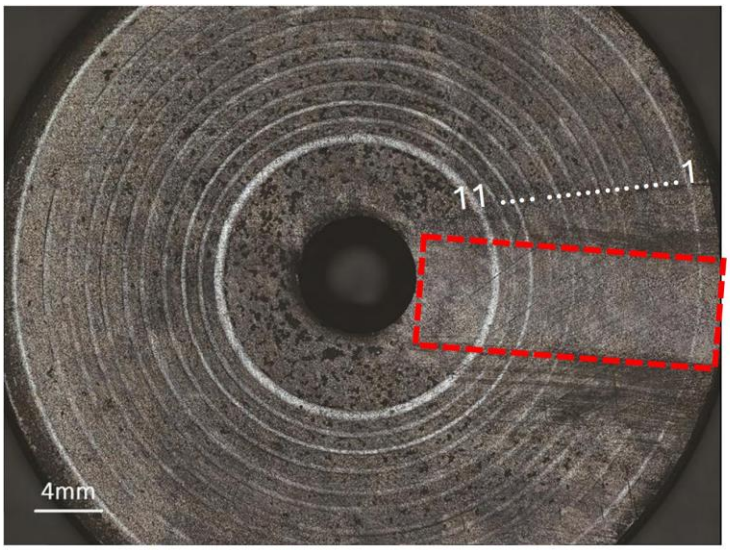
Supplementary Information

DLC disk preparation for optical profilometry



Sliding track n.	Track radius (mm)	Load (N)	Environment
1	20.5	6	Dry N_2
2	19	1	Air
3	17.5	1	Dry N_2
4	16.5	2	Dry N_2
5	15.5	2	Air
6	14.5	4	Air
7	13.5	4	Dry N_2
8	12	6	Air
9	11	6	Dry N_2
10	9.5	10	Air
11	8.5	10	Dry N_2

Fig. S1 Optical image of the functionalized DLC disk after the tribological tests. The concentric circles indicate the positions of the sliding tracks. The red dashed box outlines the area cleaned with an ethanol-soaked swab to remove the adsorbed nanomaterials, thus facilitating the reliable profilometric characterization of track morphology. The table details the lateral position, load and working environment of each sliding track.

SEM SE and BSE characterization of sliding track width

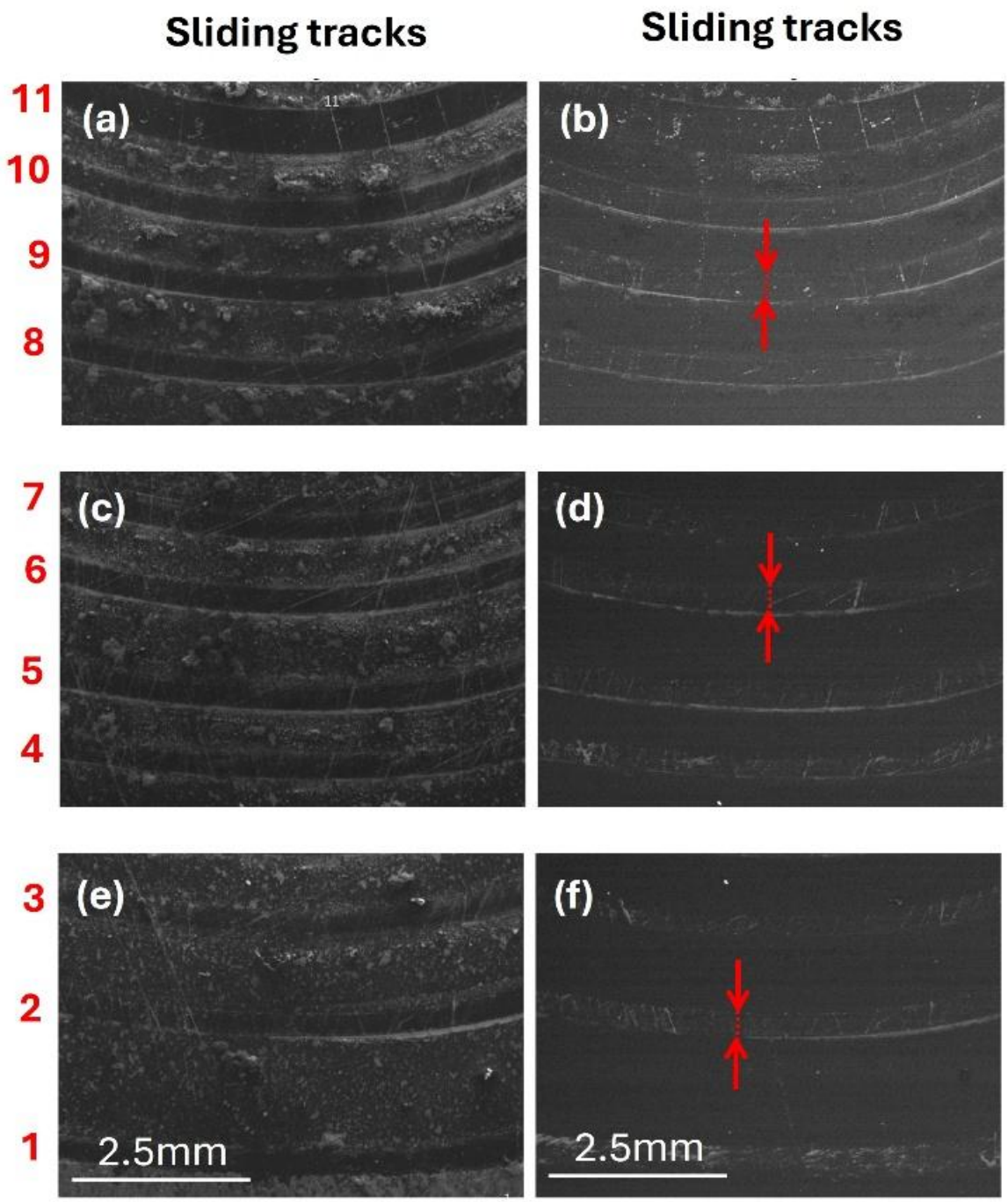


Fig. S2. SEM images of 11 sliding tracks on the functionalized DLC disk are shown in: (a, c, e) SE mode and (b, d, f) BSE mode. We estimated the effective width of each track from the BSE images (red arrows outline the width of representative tracks, measured about 20 times to provide one averaged data point in Fig. 5b), as they were less affected by the functionalized surface. The lateral position, load and working environment for each sliding track are the same of Fig. SI_1.

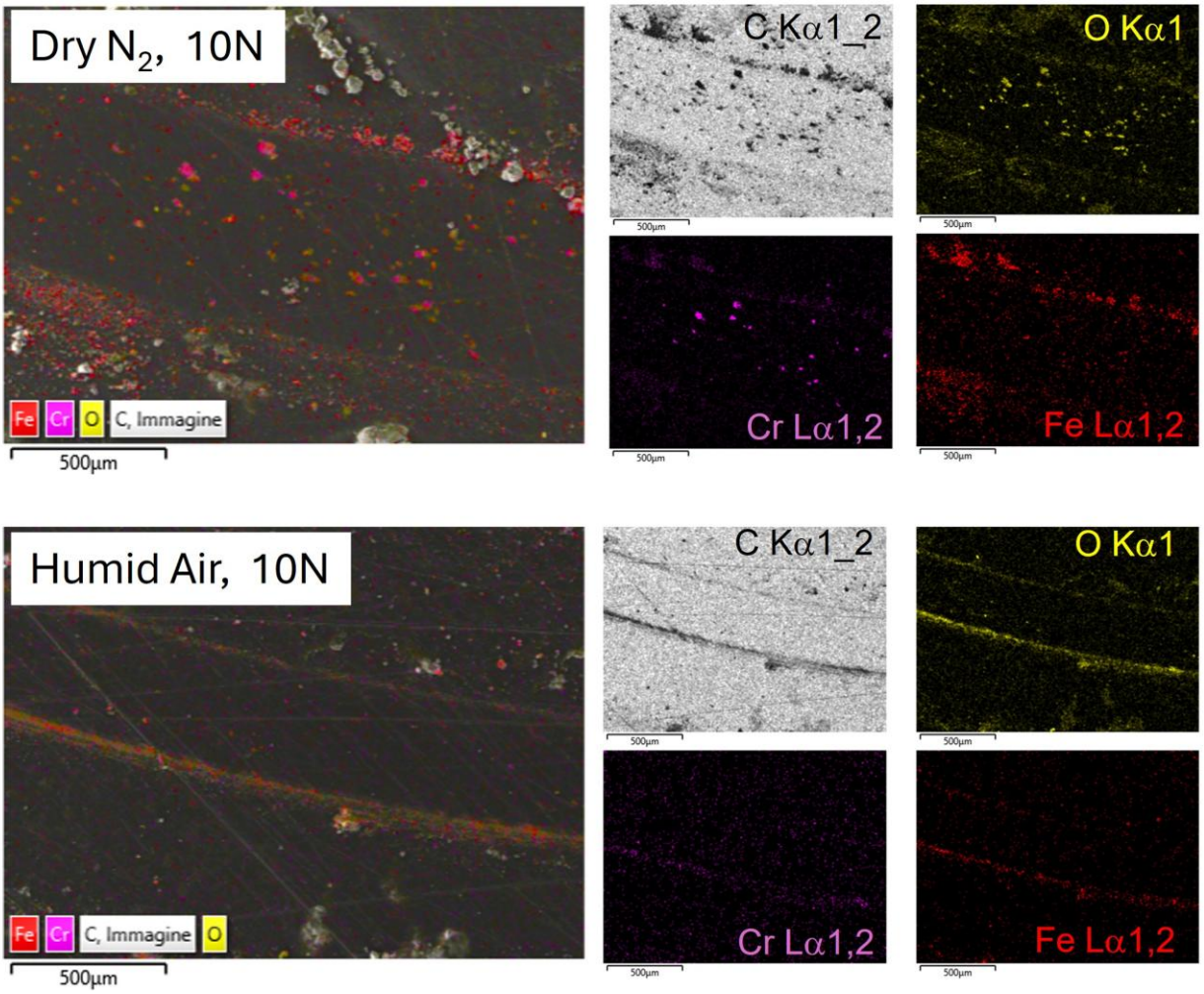


Fig. S3. SEM-EDS analysis of a GS–ND functionalized DLC surface after sliding against a SS counterpart at the maximum applied load of 10N. The left panels show SEM images of the tested regions crossed by the wear tracks, and overlaid with the elemental signals.

EDS characterization of the wear scars on the SS balls

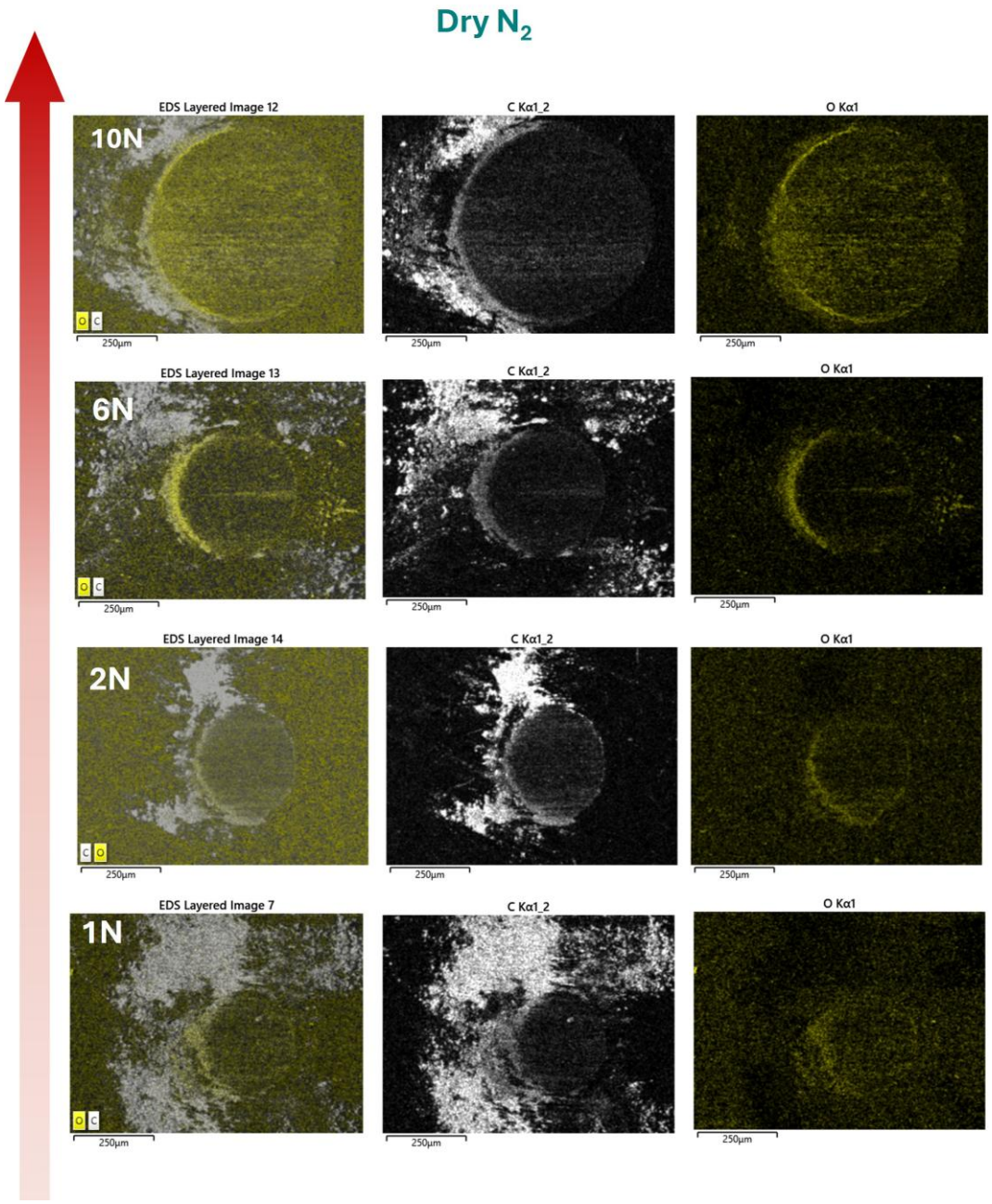


Fig. S4. EDS maps of the wear scan on the SS balls probed in dry N_2, for increasing normal loads (*indicated by the arrow from bottom to top*). In the first column, a progressive increase in the contact area with the normal load is observed. In the third column, there is evidence of mild oxidative processes at the front edge.

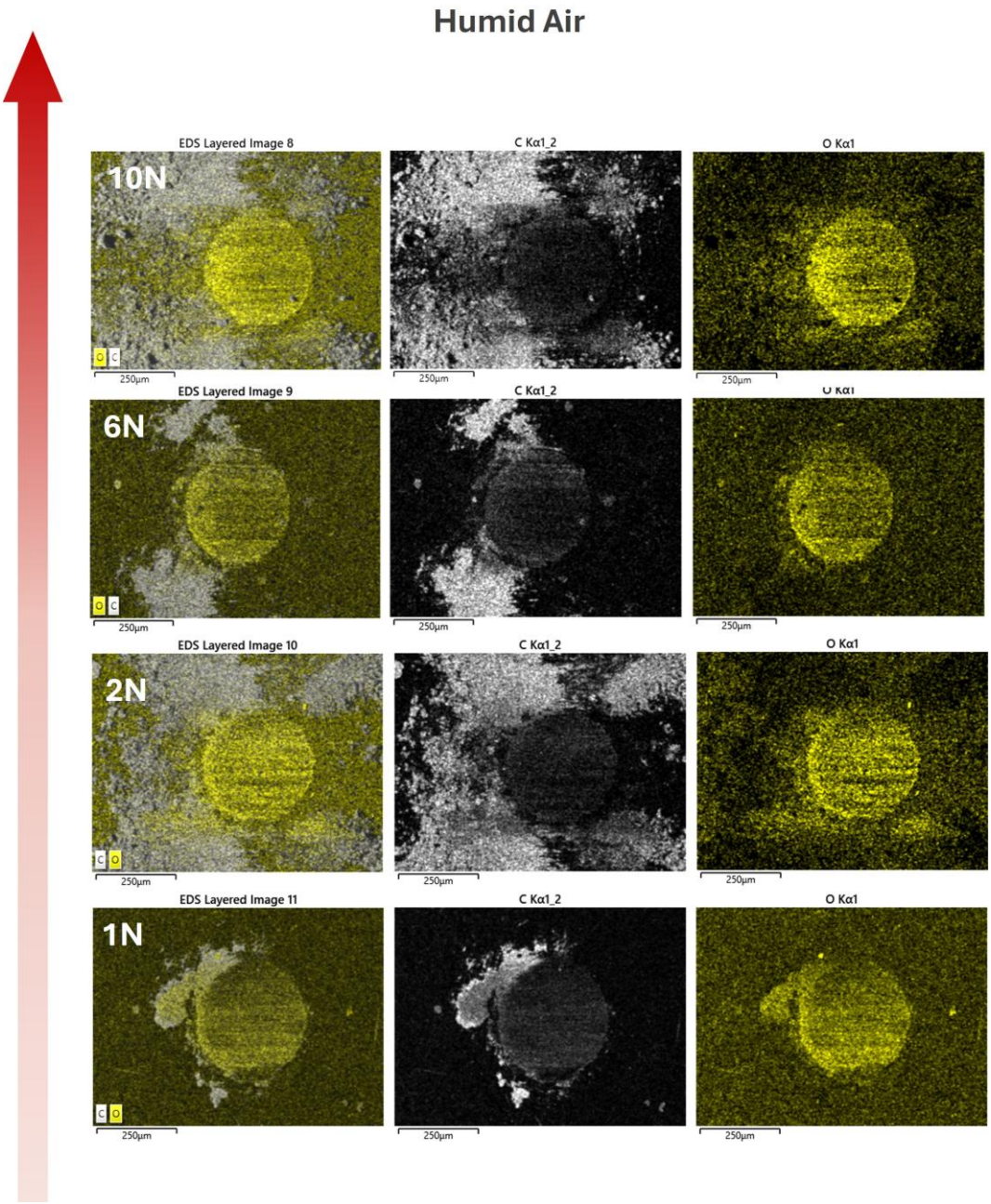


Fig. S5. EDS maps of the wear scan on the SS balls probed in humid air, for increasing normal loads (*indicated by the arrow from bottom to top*). In the first column from the left, one can see that the contact size does not evolve with the normal load. In the third column, evidence of oxidative processes is observed across the entire contact area.

	O (at.%)	Si (at.%)	Cr (at.%)	Fe (at.%)	Mo (at.%)
Unworn SS surface	1.4	0.65	17.28	80.28	0.39
1N, Dry N_2	4.68	0.47	22.09	72.28	0.48
2N, Dry N_2	4.68	0.57	22.75	71.71	0.29
6N, Dry N_2	2.12	0.09	20.27	77.11	0.41
10N, Dry N_2	7.99	0.53	20.06	71.17	0.25
1N, Humid Air	14.18	0.64	21.97	62.66	0.54
2N, Humid Air	16.65	0.65	19.62	62.76	0.32
6N, Humid Air	17.23	0.76	19.95	61.74	0.32
10N, Humid Air	18.93	0.71	19.42	60.71	0.23

Fig. S6 EDS elemental analysis of the wear scars shows how surface oxidation evolves with normal load and working environment. In dry N_2, oxidation remains mild and is restricted to the leading edge of the contact (Fig. SI_4), whereas in humid air it spreads across the entire contact area (Fig. SI_5). In such condition oxygen accounts for 14.18 – 18.93 at. %, which is at least three times higher than in dry N_2 conditions (1.40 – 4.68 at.% O). The composition measured on the unworn SS surface is consistent with the nominal AISI 440C values provided by the manufacturer.

RAMAN Analysis

The Raman spectra are described by four gaussian line-shapes arranged in two double-peak systems plus a linear background.
The amorphous carbon contributions (denoted D and G) appear as broad features (FWHM comprise between 200 and 300 cm^{-1}) while the nanodiamond-related components (denoted as D1 and G1) are sharper (FWHM comprise between 50 and 100 cm^{-1})

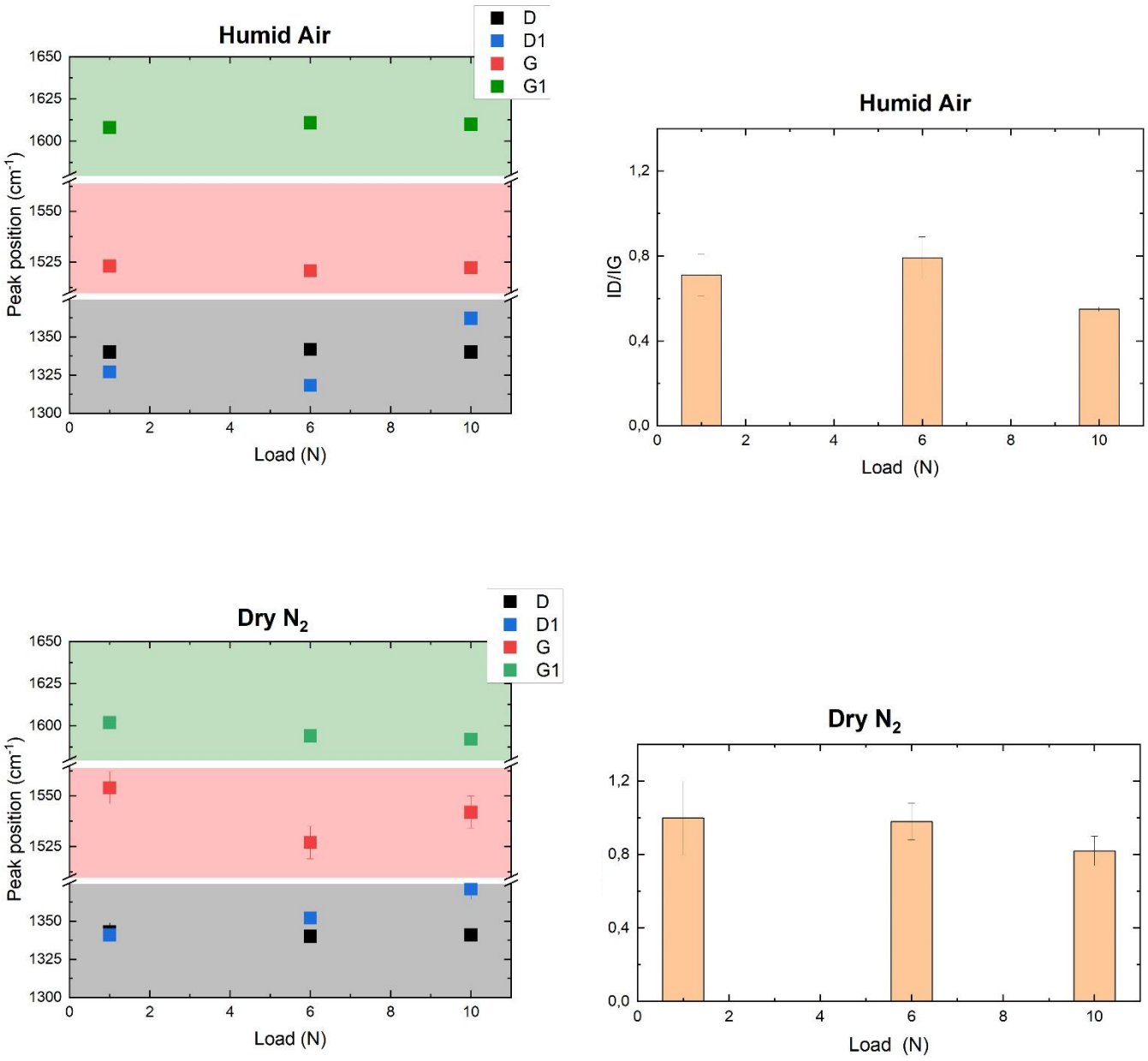


Fig. S7 Evolution of the Raman spectra contributions as a function of load in different environment; (a) peak positions in Humid Air; (b) ID/IG ratio in Humid Air; (c) peak positions in Dry N_2 ; (d) ID/IG ratio in Dry N_2